Calibration of Mold Heat Transfer Models with Breakout Shell Measurements

Junya Iwasaki1) and Brian G. Thomas2)

1) Nippon Steel Corporation, Japan.

E-mail: iwasaki.junya@nsc.co.jp

2)Department of Mechanical Science & Engineering,

University of Illinois at Urbana-Champaign, USA.

E-mail: bgthomas@uiuc.edu

This paper presents a method to calibrate a mold heat transfer model with breakout shell measurements to enable more accurate study of continuous casting of steel. A breakout shell at Nippon Steel Corporation Yawata works No.2 strand continuous caster was obtained and the shell thickness profile is measured down several vertical lines around the shell perimeter. Mold heat flux, thermocouple temperatures, gate position, mold level, casting speed and other conditions were recorded. Using a mass balance equation together with the measured data, details of the breakout were reconstructed, including the flow-rate and solidification time histories. In addition, both two- and three-dimensional finite-element models of the complex-shaped mold were developed using ABAQUS and applied to find two different offset correction factors that enable the efficient CON1D model to accurately predict temperature at both the hotface and thermocouple locations. Offset-1 accounts for the influence of slot geometry simplification in CON1D. Offset-2 accounts for the influence of thermocouple hole geometry details. As the result of the calibration, the CON1D model agrees well with both the ABAQUS models, and the plant measurements of heat flux, shell thickness, thermocouple temperatures. The model reveals new quantitative insight into the events occurring during a typical breakout, in addition to enabling better calibration parameters for future investigations.

Key Words: *continuous casting, breakout, numerical modelling*

1 Introduction

Mold heat transfer is important to internal quality, surface quality, breakout, mold life and many other aspects of the steel continuous casting process.

Mold heat transfer model CON1D[1)] is developed at the University of Illinois to understand complex mold heat transfer phenomena, improve quality, productivity, decrease cost and prevent breakout. CON1D simulates several aspects of the continuous casting process, including shell and mold temperatures, heat flux, interfacial microstructure and velocity, shrinkage estimates to predict taper, mold water temperature rise and convective heat transfer coefficient, interfacial friction, and many other phenomena. The heat transfer calculations are one-dimensional through the thickness of the shell and interfacial gap with two-dimensional conduction calculations performed in the mold. An entire simulation requires only a few seconds on a modern PC.

In order to apply CON1D model with plant, it is the most important to calibrate with plant conditions.

In this paper, calibration method of mold heat transfer with breakout shell measurements is presented to investigate solidification condition accurately, using a breakout data, such as shell thickness, thermocouple temperatures, liquid level, sliding nozzle gate position and so on, at Nippon Steel Corporation Yawata works No.2 strand continuous caster.

2 Circumstances of breakout

The breakout occurred while casting a 252 x 1360 mm slab of carbon steel, under the generally steady conditions given in **Table 1**, and 104 minutes after changing heats.

Table 1. Casting conditions

		Steel Composition	
Casting speed	23.4 mm/s		
Strand thickness	252 mm	0.16	%C
Strand width	1360 mm	0.71	%Mn
SEN submergence depth	230 mm	0.016	%P
Pour temperature	1540 °C	0.006	%S
Meniscus dist. From mold top	96 mm	0.02	%Si
Mold conductivity (WF)	242 W/mK	0.039	%Al
(NF)	355 W/mK		

Figure 1 shows the pictures of breakout shell and hole. Breakout occurred on fixed face, 30mm from north side corner, and 1200mm below the top of the shell. The size of breakout hole is about 34,000 mm^2.

Figure 2 and 3 plots several important variables as a function of time before and during the breakout. These data were measured every one second. Casting speed is constantly 1.4 m/min during over 1000 seconds before breakout. The sliding nozzle was completely closed at 0 second. The meniscus level quickly dropped and sliding nozzle was gradually opening at –22 seconds, so the start of the breakout is thought at –22sec. In

addition, meniscus level was error in signal larger than –5 seconds. Heat flux was constant at every face.

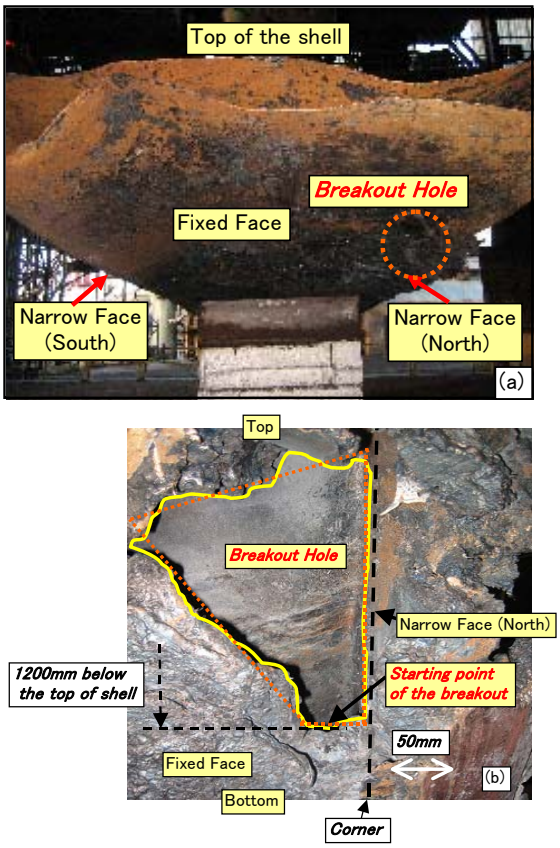

Figure 1. Breakout shell and hole
(a) Top view, (b) Enlarged photo of hole

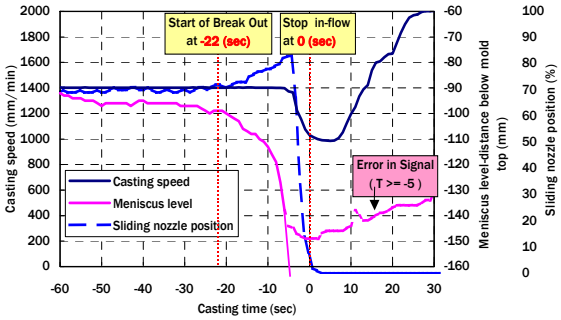

Figure 2. History of recorded casting conditions

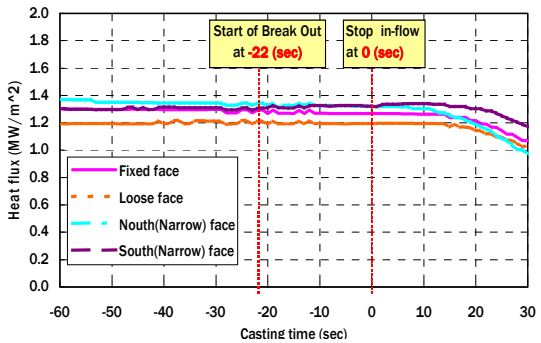

Figure 3. History of recorded heat flux

3 Estimation of flow rate and solidification time

In order to understand the solidification phenomenon of breakout shell, it is important to estimate flow rate of drop in level after breakout accurately[2]. This is to estimate solidification time at the every distance below the top of shell.

3. 1. Estimation of flow rate

The mass balance equation was established to estimate flow rate as follows.

$$Q_{in} + Q_{drop} = Q_{out} + Q_{drain} \qquad \text{.....(1)}$$

where Q_{in} is input from sliding nozzle gate, Q_{drop} is flow rate of drop in level, Q_{out} is output by casting speed and Q_{drain} is drainage from breakout hole. Eulerian reference frame based on steady-meniscus position was used in this equation. At the time before –22sec, $Q_{drain} = 0$, and after 0sec, $Q_{in} = 0$.

Figure 4 shows schematic of this mass balance equation.

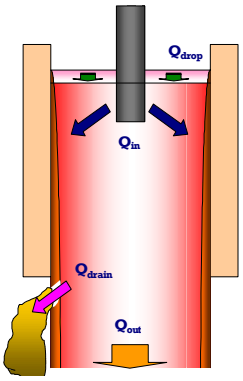

Figure 4. Schematic of mass balance

Q_{in} was approximated as a following quadratic function using real data of flow rate from sliding nozzle shown in **figure 5**.

$$Q_{in} = 0.0002X_t^2 + 0.0368X_t \qquad \text{.....(2)}$$

where X_t is sliding nozzle position at time t.

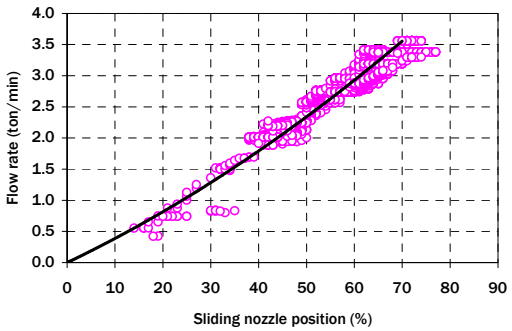

Figure 5. Real data of flow rate from sliding nozzle

Q_{out} is a function of slab width, thickness and casting speed, as follows.

$$Q_{out} = \rho \times W \times Y \times V_{C-t} \quad \text{.....(3)}$$

where ρ is steel density, W is slab width, Y is slab tickness and V_{C-t} is casting speed at time t.

In order to calculate Q_{drop} and Q_{drain}, casting time was divided into two regions. One is before –5 seconds, and another is after –5 seconds. Before –5 seconds, meniscus level was measured, so Q_{drop} could be calculated using Eqs. (4). Then Q_{drain} was given from Eqs. (1).

In addition, the breakout hole size S_t before -5 seconds was calculated at each time using Eqs. (5) to (7).

$$Q_{drop} = \rho \times W \times Y \times \frac{(z_t - z_{t-1})}{(t-(t-1))} \quad \text{.....(4)}$$

$$S_t = \frac{Q_{drain}}{\rho \times v_t} \quad \text{.....(5)}$$

$$v_t = \sqrt{2gh_{t-1}} \quad \text{.....(6)}$$

$$h_{t-1} = z_{hole-t-1} - z_{t-1} \quad \text{.....(7)}$$

where z_t and z_{t-1} are distance below steady state meniscus to liquid level at time t and t-1, v_t is speed of running fluid from berekout hole at time t, g is gravitational acceleration, h_{t-1} is liquid height from liquid level to breakout hole at time t-1 and $z_{hole-t-1}$ is distance below steady state meniscus to breakout hole at time t-1.

Figure 6 plots calculated the breakout hole sizes at every second before -5 seconds. The breakout hole sizes after -5 seconds were estimated as a exponential curve as shown Eqs. (8). The square plot in figure 6 is the measured size of the breakout hole.

$$S_t = 3713.7e^{0.2119t} \quad \text{.....(8)}$$

Q_{drop} and Q_{drain} after -5 seconds were calculated using Eqs. (1) and (4) to (8).

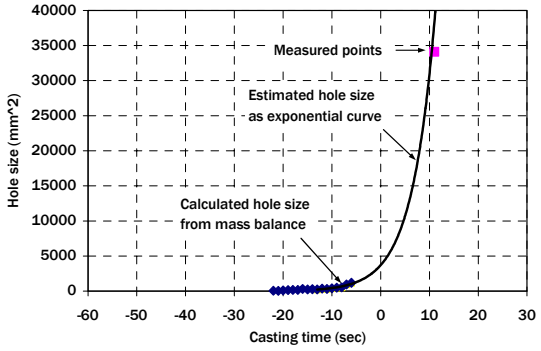

Figure 6. Calculated the breakout hole size

Figure 7 shows estimated flow rate. At –4sec, flow rate due to drop in level Q_{drop} became larger than output by casting speed Q_{out}. This means that top of the breakout shell was cast at this time. And drainage from breakout hole Q_{drain} stopped at 11sec.

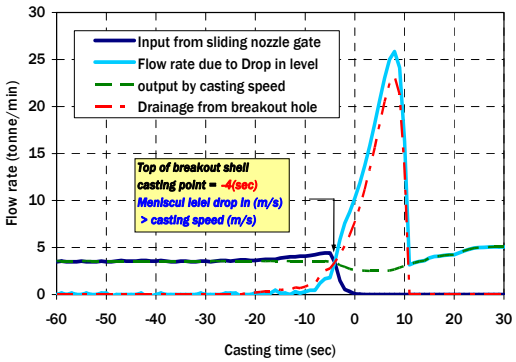

Figure 7. Calculated flow rate

3. 2. Estimated solidification time

Figure 8 illustrates the movement of the shell during the breakout. Solid lines are distance versus time histories for several points on the strand surface, which became the breakout shell. These curves were derived from the time- dependent casting speed data. The bottom of the breakout hole was cast at –59sec. And a broken line indicates liquid level.

t_{s0} is the solidification time before –4sec at L, which is a certain point below the top of the shell. And t_{s1} is the solidification time after –4sec.

t_{s0} means steady solidification time, t_{s1} means the solidification time while liquid level was dropping.

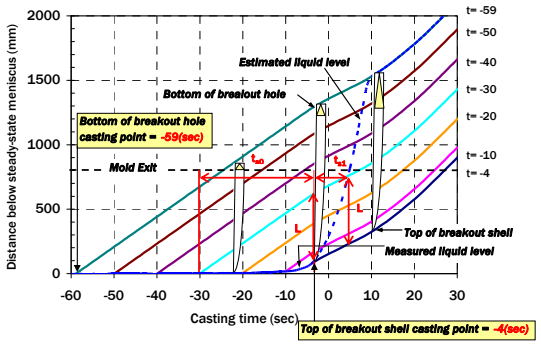

Figure 8. Distance traveled by different points on the shell surface relative to the dropping

Eqs. (9) indicates total solidification time t_s at L. And Eqs. (10) and (11) indicate the equation of t_{s0} and t_{s1}. **Figure 9** shows derived the total solidification time at the every distance below the top of shell.

These procedures explained above are the estimation method of flow rate and solidification time of the breakout.

$$t_s = t_{s0} + t_{s1} \quad \text{.....(9)}$$

$$\int_{t_{s0}}^{t_4} V_C dt = L \quad \text{.....(10)}$$

$$\int_{t_4}^{t_{s1}} \left(\frac{dz}{dt} - V_C\right) dt = L \quad \text{.....(11)}$$

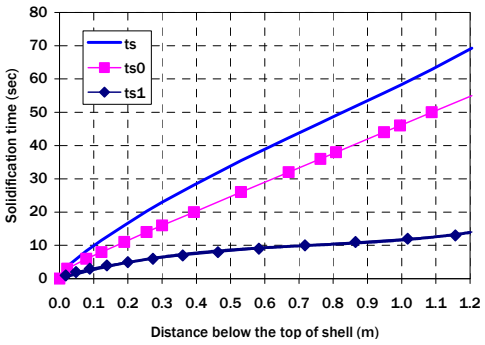

Figure 9. Solidification time

4 Heat transfer models

A finite-element model of the complex-shaped mold, developed using ABAQUS, is applied to find two different offset correction factors that enable the efficient CON1D model to accurately predict temperature at thermocouple location.

4. 1. Mold geometry simplification with CON1D

Figure 10 shows the actual wide face mold geometry. The actual water channels are 5 mm wide by 13 mm deep with rounded roots. In order to create the simple mold geometry for CON1D, water channel was transformed into the one dimensional rectangular channel geometry, as shown in **figure 11**. The CON1D water channels are 5 mm wide but only 12.46 mm deep, so that the cross area equals that of the actual channel.

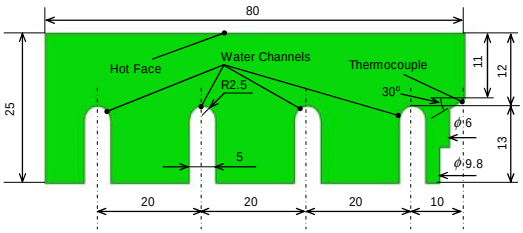

Figure 10. Wide face mold geometry

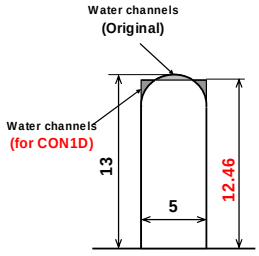

Figure 11. Wide face water channel & CON1D simplification

4. 2. CON1D model offset determination with ABAQUS

4. 2. 1. Procedure of offset

Figure 12 indicates the procedure of CON1D model offset determination with ABAQUS.

Offset-1 is the offset for the influence of heat transfer difference between con1d and ABAQUS-2D model. This method is established newly in this research.

Offset-2 is the offset for the influence of thermocouple hole geometry. This method was already published and applied this method in this research.

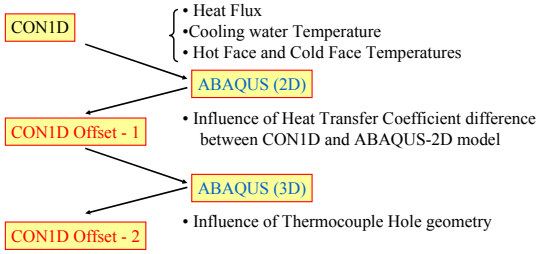

Figure 12. Procedure of offset

4. 2. 2. Offset-1 – Influence of mold heat transfer difference between CON1D and ABAQUS-2D model

In CON1D, water channels are thought as fin as shown **Figure 13**, so the heat transfer coefficient between water and the side of the water channels is calculated assuming fin flow, as shown Eqs. (12) and (13).

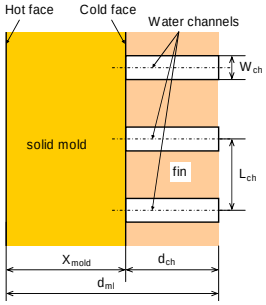

Figure 13. CON1D model – water channel-

$$h_{water} = 1/\left(\frac{d_{scale}}{k_{scale}} + \frac{1}{h_{fin}}\right) \quad \text{.....(12)}$$

$$h_{fin} = \frac{h_w w_{ch}}{L_{ch}} + \frac{\sqrt{2h_w k_{mold}\left(L_{ch} - w_{ch}\right)}}{L_{ch}} \times \tanh\sqrt{\frac{2h_w d_{ch}^2}{k_{mold}\left(L_{ch} - w_{ch}\right)}} \quad \text{...(13)}$$

where h_{water} is heat transfer coefficient using CON1D, d_{scale} is scale thickness of water scale at mold cold face, k_{scale} is conductivity of water scale at mold cold face,

h_w is heat transfer coefficient between water and sides of water channels which is used for ABAQUS-2D and 3D models as follows, k_{mold} is conductivity of mold, and L_{ch}, w_{ch} and d_{ch} are geometry parameters shown in Figure 13.

While in ABAQUS, the heat transfer coefficient was calculated assuming turbulent flow through a pipe, as shown Eqs. (14) to (24).

This difference causes the mold heat transfer difference between CON1D and ABAQUS. Therefore, the calibration using offset-1 is needed.

$$h_w = \frac{k_{waterm}}{D}\left(5 + 0.015\,\mathrm{Re}_{waterf}^{c_1}\,\mathrm{Pr}_{waterw}^{c_2}\right) \quad \text{.....(14)}$$

$$D = \frac{2W_{ch}d_{ch}}{W_{ch}+d_{ch}} \quad \text{.....(15)}$$

$$c_1 = 0.88 - 0.24/\left(4+\mathrm{Pr}_{waterw}\right) \quad \text{.....(16)}$$

$$c_2 = 0.333 + 0.5e^{-0.6\,\mathrm{Pr}_{waterw}} \quad \text{.....(17)}$$

$$\mathrm{Re}_{waterf} = \frac{\rho_{water} v_{water} D}{\mu_{waterf}} \quad \text{.....(18)}$$

$$\mathrm{Pr}_{waterw} = \frac{\mu_{waterw} Cp_{water}}{k_{waterw}} \quad \text{.....(19)}$$

$$k_{waterm} = 0.59 + 0.001T_{water} \quad \text{.....(20)}$$

$$k_{waterw} = 0.59 + 0.001T_{cold} \quad \text{.....(21)}$$

$$\mu_{waterf} = 2.062*10^{-9}\rho_{water}*10^{\left(\frac{792.42}{T_{film}+273.15}\right)} \quad \text{...(22)}$$

$$\mu_{waterw} = 2.062*10^{-9}\rho_{water}*10^{\left(\frac{792.42}{T_{cold}+273.15}\right)} \quad \text{...(23)}$$

$$T_{film} = 0.5(T_{water} + T_{cold}) \quad \text{.....(24)}$$

where k_{water} is conductivity of water, μ_{water} is water viscosity, v_{water} is cooling water velocity, ρ_{water} is water density, Cp_{water} is water heat capacity, T_{water} is cooling water temperature and T_{cold} is cold face temperature.

Figure 14 shows boundary conditions and properties of wide face with ABAQUS. And **Figure 15, 16** show analyzed results. The temperature difference between CON1D and ABAQUS-2D analysed results ΔT_{hot} is defined as shown Eqs. (25) and the value is 8.0 °C at the hot face. And offset-1 is defined as shown Eqs. (26) and the value is 1.34mm.

$$\Delta T_{hot} = \frac{\left(T_{hot-path1} - T_{hot-path2}\right)}{2} - T_{hot-CON1D} \quad \text{...(25)}$$

$$d_{offset-1} = \Delta T_{hot}\frac{dx}{dT} \quad \text{.....(26)}$$

where T_{hot} is hot face temperature.

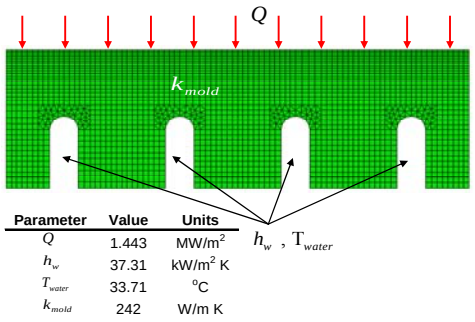

Parameter	Value	Units
Q	1.443	MW/m^2
h_w	37.31	kW/m^2 K
T_{water}	33.71	°C
k_{mold}	242	W/m K

Figure 14. Boundary conditions and properties

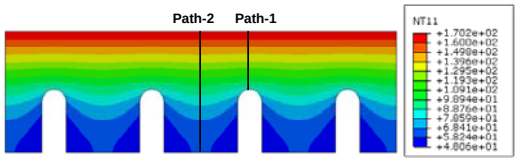

Figure 15. Analyzed result (ABAQUS-2D)

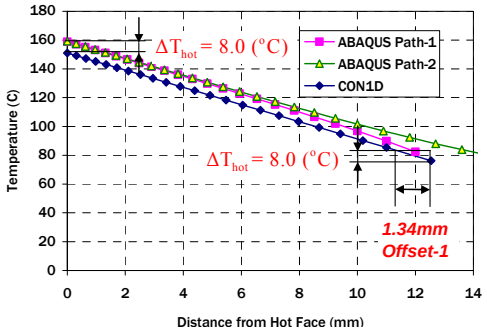

Figure 16. Temperature profiles in wide face

Figure 17 shows temperature profile with offset-1. The profile of CON1D with offset-1 agrees well with ABAQUS-2D profile.

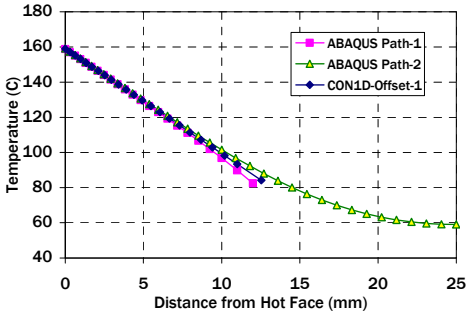

Figure 17. Temperature profiles with offset-1

Next, offset-1 was generalized by water channel geometry. **Figure 18** shows relation of distance between water channel to hot face temperature with CON1D and ABAQUS-2D. Horizontal axis is distance between water channel and vertical axis is hot face temperature. Case 1 is thinner mold thickness than case

2 and two different heat fluxes are calculated in each case.

In these every case, temperature difference increased as distance between water channels increased.

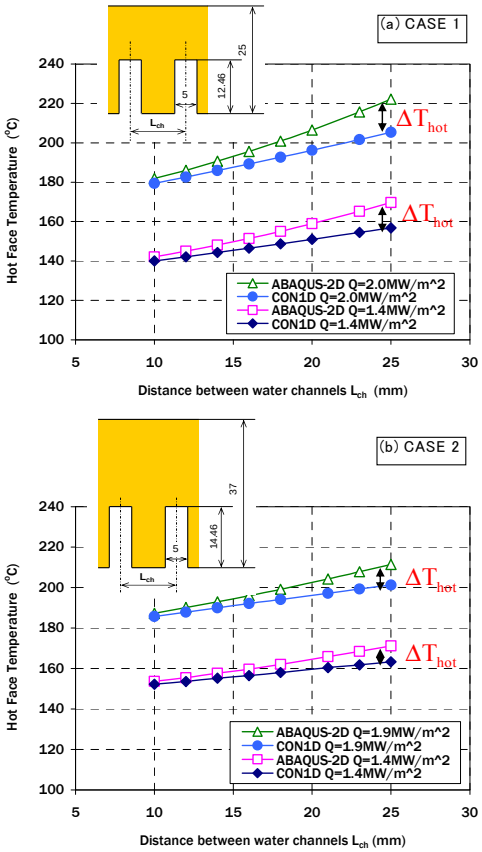

Figure 18. Relation of distance between water channel to hot face temperature with CON1D and ABAQUS-2D

Figure 19 shows relation of water channel geometry parameter X to offset-1. Water channel geometry parameter X was calculated using Eqs. (27) and (15).

This relation was approximated power curve as shown Eqs. (28).

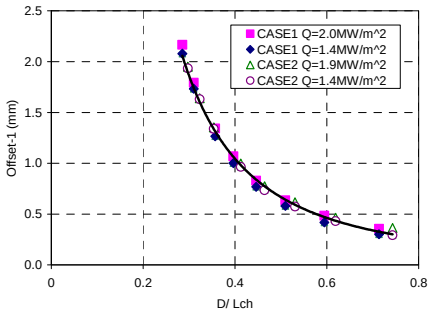

Figure 19. Relation of water channel geometry parameter X to offset-1

$$X = \frac{D}{L_{ch}} \qquad \text{.....(27)}$$

$$d_{offset-1} = 0.1659 X^{-2.0083} \qquad \text{.....(28)}$$

Figure 20 shows error of hot face temperature between CON1D generalized offset-1 to ABAQUS. The errors are within 1 °C. Therefore, offset-1 can be calculated using these equations.

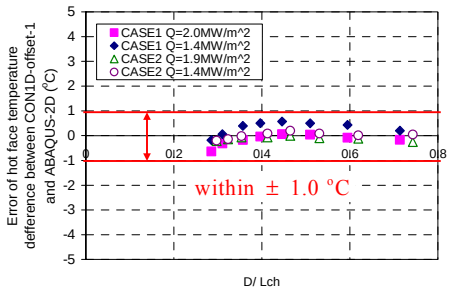

Figure 20. Error of hot face temperature between CON1D-generalized offset-1 to ABAQUS-2D

4. 2. 3. Offset-2 – Influence of thermocouple hole Geometry

To enable CON1D to accurately predict the thermocouple temperatures, calibration method, using a three-dimensional heat transfer calculation to determine an offset-2 distance for each mold face to adjust the modeled depth of the thermocouples,[3] is applied.

Figure 21 shows wide face boundary conditions and properties with ABAQUS-3D.

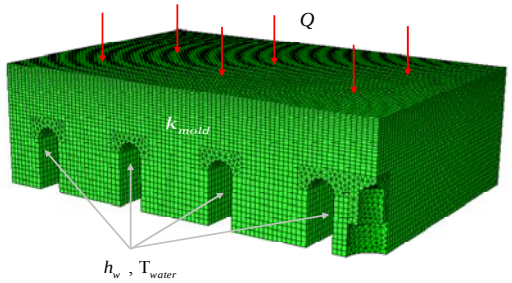

Parameter	Value	Units
Q	1.443	MW/m^2
h_w	37.31	kW/m^2 K
T_{water}	33.71	°C
k_{mold}	242	W/m K

Number of elements : 196598
(hexahedrons, tetrahedrons)

Figure 21. Wide face boundary conditions and properties with ABAQUS-3D

Figure 22, 23 show analyzed results. Offset-2 is given as shown Eqs. (29). In this case, offset-2 is 1.61mm as shown Figure 24.

$$d_{offset-2} = \left(T_{TC} - T_{hf}\right)\frac{dx}{dT} - d_{TC} \qquad \text{.....(29)}$$

where T_{TC} is thermocouple temperature from ABAQUS, T_{hf} is thermocouple temperature from CON1D dx/dT is inverse of the temperature gradient from CON1D, and d_{TC} is the actual depth of the thermocouple from the hot face.

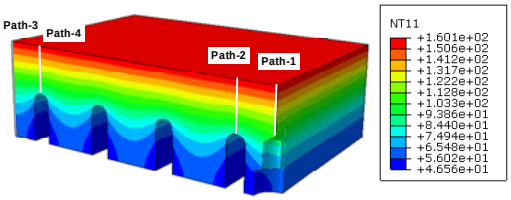

Figure 22. Analyzed result (ABAQUS-3D)

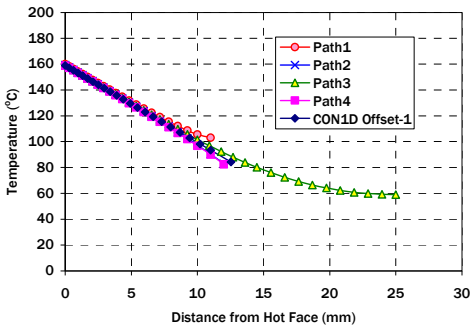

Figure 23. Temperature profiles in wide face

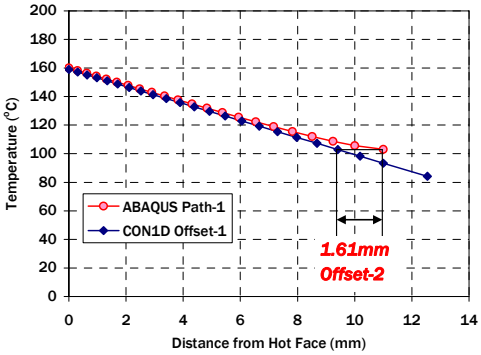

Figure 24. Determination of offset-2

5 CON1D model verification with plant

CON1D model using calibration explained above is verified with plant data.

Table 2 shows the CON1D fitting conditions. Fitting parameters are solid and liquid flux conductivity, slag rim thickness, cold face scale thickness and constant ratio of solid flux velocity to casting speed.

In this condition, CON1D predicted mean heat flux in the mold agrees with the plant data.

Table 2. CON1D fitting conditions

	Fixed face	Narrow face
Simulation shell	Fixed face	
Casting speed	23.4 mm/s	
SEN submergence depth	230 mm	
Pour temperature	1540 ℃	
Meniscus dist. From mold top	96 mm	
Fraction solid for shell thickness location	0.35	
Treatment of superheat	-	1 : default
Mean heat flux in mold - measured	1.279 MW/m^2	1.294 MW/m^2
Fitting Parameters		
- Solid flux conductivity	1.00 W/mK	
- Liquid flux conductivity	1.00 W/mK	
- Location of peak heat flux	-	0.03 m
- Slag rim thickness at metal level	-	2.20 mm
- Slag rim thickness at heat flux peak	-	0.75 mm
- Cold face scale thickness	-	0.002mm
- Constant ratio of solid flux velocity to casting speek	0.085	0.084
CON1D prediction		
- Mean heat flux in mold	1.279 MW/m^2	1.293 MW/m^2

Figure 25 shows CON1D calculated shell thickness profiles. Eqs. (30) to (33) are the approximated equation of shell thickness profiles. These equations and solidification time explained above are used to calculate shell thickness of breakout shell.

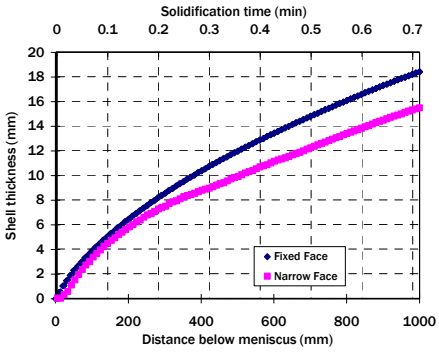

Figure 25. CON1D calculated shell thickness profile

Wide face

$$t_s \le 0.04$$
$$S_t = 54.763 t_{sol} + 1.9306 t_{sol}^{0.5} \quad \text{.....(30)}$$
$$t_s > 0.04$$
$$S_t = 25.244 t_{sol}^{0.5} - 3.0216 \quad \text{.....(31)}$$

Narrow face

$$t_s \le 0.01$$
$$S_t = 0 \quad \text{.....(32)}$$
$$t_s > 0.01$$
$$S_t = 20.604 t_{sol}^{0.5} - 2.1854 \quad \text{.....(33)}$$

where t_s is total solidification time and S_t is shell thickness.

Figure 26 shows comparison between CON1D calculated profiles and measurements from breakout shell. The shell thickness of breakout condition is thicker than that of steady casting because of additional solidification time while liquid level was dropping. The

calculated profiles with CON1D for breakout condition agree well with measured profiles.

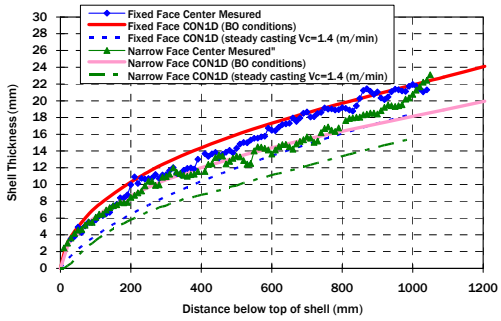

Figure 26. Comparison between CON1D calculated profile and measurements from BO shell

Figure 27, 28 shows thermocouple temperatures comparison between CON1D with total offset and measured data in wide face and narrow face. Total offset is offset-1 plus offset-2 as shown Eqs. (34).

Table 3 indicates thermocouple temperature differences between CON1D calculated data and plant data in wide and narrow face. CON1D calculated temperature agree well with plant data within 8.2 ^{o}C.

$$d_{offset} = d_{offset-1} + d_{offset-2} \quad \text{.....(34)}$$

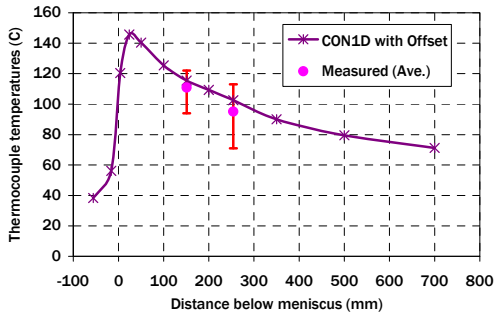

Figure 27. Thermocouple temperatures comparison between CON1D and mesured data in wide face

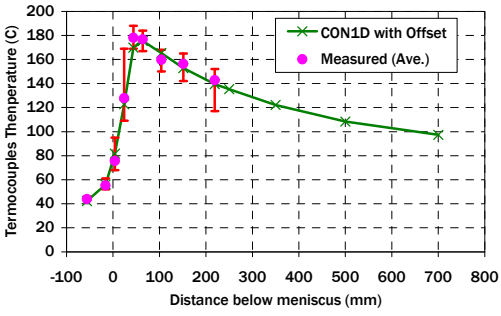

Figure 28. Thermocouple temperatures comparison between CON1D and mesured data in narrow face

Table 3. Thermocouple temperature comparison

	Distance below Meniscus	Measured (Ave.) Temperature	CON1D with offset Temperature	CON1D with offset Difference
	mm	^{o}C	^{o}C	^{o}C
Wide Face	151.5	110.9	115.43	**4.5**
	254.0	95.1	102.61	**7.5**
Narrow Face	-56	43.9	42.21	**-1.6**
	-16.0	55.2	56.08	**0.8**
	4.0	75.5	81.65	**6.1**
	24.0	127.8	122.66	**-5.2**
	44.0	178.1	169.86	**-8.2**
	64.0	176.7	175.35	**-1.3**
	104.0	159.7	165.46	**5.7**
	151.5	156.4	152.75	**-3.6**
	219.0	142.8	139.57	**-3.2**

6 Conclusions

- A mass balance equation to derive the flow rate history and solidification time of a breakout shell is developed, and applied to understand events during a real breakout.
- General formula of calibration of offset parameters are established and applied.
- Calculated shell thickness agrees well with CON1D and with the measured thickness of the breakout shell.
- Thermocouple temperatures calculated with CON1D using the new offsets agree well with plant measurements (within 8.2 ^{o}C).

Acknowledgment

The authors would like to thank the member companies of Continuous Casting Consortium at the University of Illinois and personnel at Nippon Steel Corporation at Yawata works for plant data and support.

References

(1) Y. Meng and B. G. Thomas: Metall Mater Trans B. 34B (2003). No. 5. 685

(2) B.G. Thomas, R. O'Malley and D. Stone: TMS, Warrendale, PA, 1998, pp.1185-1199

(3) B. Santillana, L. C. Hibbeler, B. G. Thomas, A. Hamoen, A. Kamperman and W. V. D. Knoop: ISIJ Int.. 48 (2008). No. 10. 1380